

# We are IntechOpen, the world's leading publisher of Open Access books Built by scientists, for scientists

6,900

Open access books available

186,000

International authors and editors

200M

Downloads

Our authors are among the

154

Countries delivered to

TOP 1%

most cited scientists

12.2%

Contributors from top 500 universities



WEB OF SCIENCE™

Selection of our books indexed in the Book Citation Index  
in Web of Science™ Core Collection (BKCI)

Interested in publishing with us?  
Contact [book.department@intechopen.com](mailto:book.department@intechopen.com)

Numbers displayed above are based on latest data collected.  
For more information visit [www.intechopen.com](http://www.intechopen.com)



# The Influence of the Hydrodynamic Conditions on the Performance of Membrane Distillation

Marek Gryta

*West Pomeranian University of Technology, Szczecin  
Poland*

## 1. Introduction

Membrane distillation (MD) is an evaporation/condensation process of volatile components through a hydrophobic porous membrane. The maintenance of gas phase inside the membrane pores is a fundamental condition required to carry out the MD process. A hydrophobic nature of the membrane prevents liquid penetration into the pores. Membranes having these properties are prepared from polymers with a low value of the surface energy, such as polypropylene (PP), polytetrafluoroethylene (PTFE) or polyvinylidene fluoride (PVDF) (Alklaibi & Lior, 2005; Bonyadi & Chung, 2009, Gryta & Barancewicz, 2010). Similar to other distillation processes also MD requires energy for water evaporation. The hydrodynamic conditions occurring in the membrane modules influence on the heat and mass transfers, and have a significant effect on the MD process efficiency.

The MD separation mechanism is based on vapour/liquid equilibrium of a liquid mixture. For solutions containing non-volatile solutes only the water vapour is transferred through the membrane; hence, the obtained distillate comprises demineralized water (Alklaibi & Lior, 2004; Gryta, 2005a; Schneider et al., 1988). However, when the feed contains various volatile components, they are also transferred through the membranes to the distillate (El-Bourawi et al., 2006; Gryta, 2010a; Gryta et al., 2006a). Based on this separation mechanism, the major application areas of MD include water treatment technology, seawater desalination, production of high purity water and the concentration of aqueous solutions (El-Bourawi et al., 2006; Drioli et al., 2004, Gryta, 2006a, 2010b; Karakulski et al., 2006; Martínez-Díez & Vázquez-González, 1999; Srisurichan et al., 2005; Teoh et al., 2008).

A few modes of MD process are known: direct contact membrane distillation (DCMD), air gap membrane distillation (AGMD), sweeping gas membrane distillation (SGMD), vacuum membrane distillation (VMD) and osmotic membrane distillation (OMD). These variants differ in the manner of permeate collection, the mass transfer mechanism through the membrane, and the reason for driving force formation (Alklaibi & Lior, 2005; Gryta, 2005a).

The most frequently studied and described mode of MD process is a DCMD variant. In this case the surfaces of the membrane are in a direct contact with the two liquid phases, hot feed and cold distillate (Fig. 1). The DCMD process proceeds at atmospheric pressure and at temperatures that are much lower than the normal boiling point of the feed solutions. This allows the utilization of solar heat or so-called waste heat, e.g. the condensate from turbines or heat exchangers (Banat & Jwaied, 2008; Bui et al., 2010; Li & Sirkar, 2004).

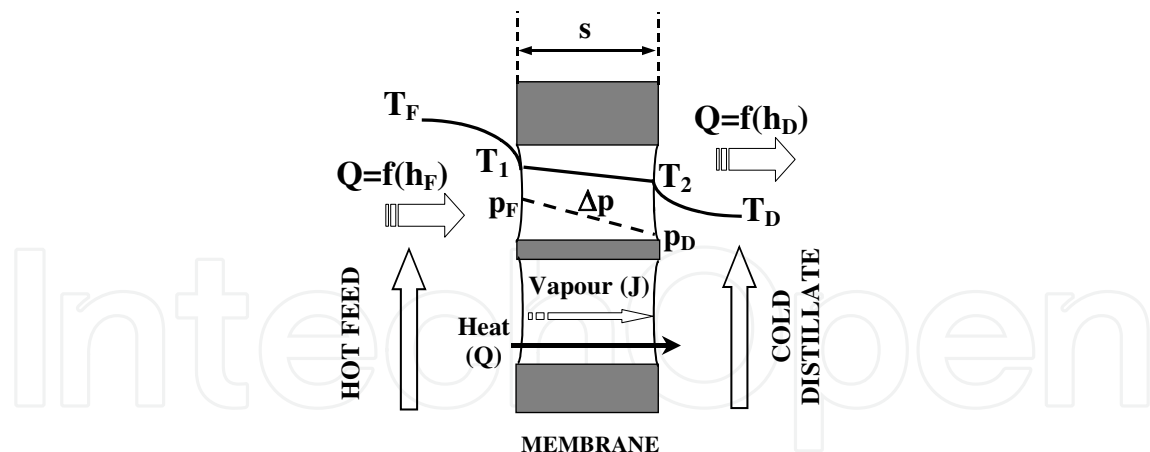


Fig. 1. Principles of DCMD:  $T_1$ ,  $T_2$ ,  $T_F$ ,  $T_D$  – temperatures at both sides of the membrane, and temperatures of feed and distillate, respectively;  $p_F$ ,  $p_D$  and  $h_F$ ,  $h_D$  – water vapor partial pressure and heat transfer coefficients at the feed and distillate sides, respectively

The driving force for the mass transport in DCMD is a difference of the vapour pressure ( $\Delta p$ ), resulting from different temperatures and compositions of solutions in the layers adjacent to the membrane (Fig. 1). The stream parameters (temperature, concentration) at the solution/membrane interface differ significantly from those in the bulk, as a result of the polarization phenomena associated with both the temperature and concentration. These phenomena cause a decrease in the vapour pressure difference across the membrane which in turn leads to the reduction of the permeate flux in the MD process. Therefore, the hydrodynamic conditions have a pronoun influence on the efficiency of the MD process (Alklaibi & Lior, 2005; Gryta, 2002a, 2005a, 2005b; Gryta et al., 2000; Martínez-Díez & Vázquez-González, 1999; Li & Sirkar, 2004).

The feed temperature in the MD module decreases due to evaporation, which also causes a reduction of MD driving force, in addition to the temperature polarisation. Therefore, the permeate flux can be increased several times when the flow rate and temperature of the feed is enhanced in an appropriate way. Moreover, the shape and dimensions of the channels through which liquid flows in the module has an important effect on the permeate flux (Gryta et al., 2000; Schneider et al., 1988; Teoh et al., 2008).

The efficiency of MD process depends, in a significant degree, on the morphology of used membranes. The permeate flux increases along with an increase in membrane porosity and pore diameter (El-Bourawi et al., 2006). The higher the wall thickness of membrane, the larger the diffusion resistance. Therefore, a larger efficiency can be achieved for thinner membranes. However, the thick membranes undergo mechanical damage more easily, and, the manner of their assembly in the MD module plays an essential role (Gryta et al., 1997).

## 2. Heat and mass transfer in MD process

In the MD process both heat and mass transfer occur simultaneously, therefore, both temperature and concentration polarization effects should be taken into consideration. A number of theoretical models have been developed for the description of the membrane distillation (Alklaibi & Lior, 2005; El-Bourawi et al., 2006; Gryta, 2002b, 2008; Gryta et al., 1997, 1998; Lawson & Lloyd, 1997; Li & Sirkar, 2004; Martínez-Díez & Vázquez-González, 1999). The models of direct contact MD were based on the assumption that vapour

permeates through the porous membrane, as a result of the molecular diffusion, Knudsen flow and/or the transition between them. The permeate flux can be described by:

$$J = \frac{\varepsilon}{\chi} \frac{M}{s RT_m} D_{WA} P \ln \frac{P - p_D}{P - p_F} \quad (1)$$

where  $p_F$  and  $p_D$  are the partial pressures of saturated water vapour at temperatures  $T_1$  and  $T_2$  (Fig. 1), and  $\varepsilon$ ,  $\chi$ ,  $s$ ,  $T_m$  are the porosity, tortuosity, thickness, and mean temperature of the membrane, respectively, and  $M$  is the molecular weight of water,  $R$  is the gas constant,  $P$  is the total pressure, and  $D_{WA}$  is the effective diffusion coefficient of water vapour through the membrane pores. The vapour pressure of water for the diluted solutions can be determined e.g. from the Antoine equation (Gryta et al., 1998). However, for concentrated solutions the effect of solute concentration on the partial vapour pressure it should be taken into account. The literature offers a considerable number of equations and the experimental data, which can be used to solve this problem.

The temperatures in the layers adjacent to the membrane ( $T_1$ ,  $T_2$ ) are dependent on the values of the heat transfer coefficients in the MD module (Gryta et al., 1997, 1998). The values of these coefficients increase along an increase of the flow rates, thus, the temperature polarization can be considerably reduced by the application of high flow rates. Moreover, a higher flow rate decreases the temperature difference of streams at the inlet and outlet of the module, resulting in the increase of the temperature difference across the membrane.

The temperatures  $T_1$  and  $T_2$  cannot be measured directly. A series of equations for their calculations have been presented in the MD literature (Alklaibi & Lior, 2005; Gryta et al., 1997, 1998; Khayet et al., 2004; Lawson & Lloyd, 1997; Schofield et al., 1990). These equations were derived for the steady state conditions, under which the amount of heat transferred to and from the surfaces adjacent to the membrane is equal to the amount of heat transferred inside the membrane. For the case presented in Fig. 1 we can write:

$$Q = h_F(T_F - T_1) = J \Delta H + \frac{\lambda_m}{s}(T_1 - T_2) = h_D(T_2 - T_D) = H(T_F - T_D) \quad (2)$$

A solution of the above equations allows to determine the temperatures  $T_1$  and  $T_2$  - Eqs. 2 and 3. These equations were derived with the assumption of the linear temperature change in the membrane and isoenthalpic flow of vapour (Gryta et al., 1998).

$$T_1 = \frac{\frac{\lambda_m}{s} \left( T_D + \frac{h_F}{h_D} T_F \right) + h_F T_F - J \Delta H}{\frac{\lambda_m}{s} + h_F \left( 1 + \frac{\lambda_m}{h_D s} \right)} \quad (3)$$

$$T_2 = \frac{\frac{\lambda_m}{s} \left( T_F + \frac{h_D}{h_F} T_D \right) + h_D T_D + J \Delta H}{\frac{\lambda_m}{s} + h_D \left( 1 + \frac{\lambda_m}{h_F s} \right)} \quad (4)$$

where  $\Delta H$  is the vapour enthalpy,  $H$  and  $h_i$  are the overall and convective heat transfer coefficients, and  $\lambda_m$  is the membrane thermal conductivity. The  $h_i$  coefficients can be estimated from the Nusselt number:  $Nu = h_i d_h / \lambda$ , where  $d_h$  is the hydraulic diameter and  $\lambda$  is the thermal conductivity of liquid.

The thermal conductivity coefficient for membranes utilized in MD changes in a small range of 0.04–0.06 W/mK, and it can be determined on the basis of the membrane material data (Phattaranawik et al., 2003):

$$\lambda_m = \lambda_g \varepsilon + (1 - \varepsilon) \lambda_s \quad (5)$$

The convective heat-transfer coefficient ( $h_i$ ) can vary in a wide range, depending on the design and working conditions of the MD module. Thus, the accurate determination of its value has an essential meaning. The coefficients  $h_D$  and  $h_F$  can be calculated from equation:

$$h_i = \frac{Nu \lambda_i}{d_h} \quad (6)$$

The Nusselt number occurring in this equation is most often determined from the following correlation:

$$Nu = C Re^a Pr^b \left( \frac{d_h}{L} \right)^c \quad (7)$$

where  $C$ ,  $a$ ,  $b$ ,  $c$  are the coefficients depending on a channel configuration of the heat exchanger and a flowing character of the streams. Nusselt number correlations developed for the heat exchangers can be used for heat transfer calculations in MD modules. However, care must be taken in the selection of the appropriate correlation. The  $Nu$  correlations selected for the tubular exchanger were also applied successfully for the model calculation of MD process in the capillary module. For a MD module with the membranes arranged in a form of braided capillaries the following form of the Nusselt number was successfully used for laminar flow (Gryta et al., 1998):

$$Nu = 4.36 + \frac{0.036 \times Pe \times \frac{d_h}{L}}{1 + 0.0011 \times \left( Pe \times \frac{d_h}{L} \right)^{0.8}} \quad (8)$$

where  $L$  is the module length, the Peclet number ( $Pe$ ) is given by the equation  $Pe = Pr Re$ , the Prandtl number ( $Pr$ ) is  $Pr = c_{ps} \mu / \lambda$ , the Reynolds number ( $Re$ ) is  $Re = v d_h \rho / \mu$  and  $\mu$ ,  $\rho$ ,  $c_{ps}$ , are the viscosity, density and the specific heat of solution, respectively.

## 2.1 MD process parameters

The feed stream temperature has a significant effect on the level of permeate flux in the MD process (Fig. 2). At constant distillate temperature (293 K) the elevation of  $T_F$  from 333 K to 358 K caused an increase in the permeate flux by about 100-200% (Wang et al, 2008). The presented results confirmed that a high efficiency in the MD process could be achieved when the feed temperature is close to the boiling point. Such a high increase of the flux can

be explained by an exponential dependence of the vapour pressure on temperature (Fig. 2 – broken line). Thus, the driving force for the mass transfer also increases with increasing the feed temperature. Increasing the distillate temperature causes the reverse effect, i.e. declines of permeate flux. However, the changes of permeate flux are not so pronounced as in the case of feed temperature variation. As a results of the exponential function  $\Delta p=f(T)$  considerably large changes of  $\Delta p$  were achieved for the feed (e.g. from 333 to 358 K) than for distillate (e.g. from 293 to 318 K) (Gryta, 2002b; Gryta et al., 2000).

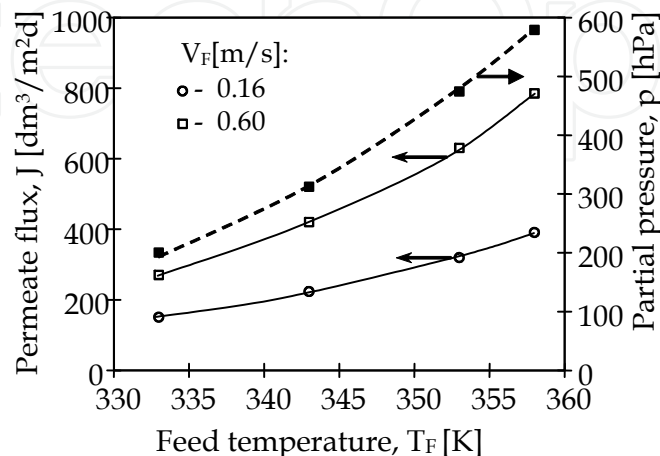


Fig. 2. The influence of feed temperature on the permeate flux and water vapour pressure. Capillary Accurel PP S6/2 membrane, module length 0.6 m, counter-current flow,  $T_D=293$  K

The results presented in Figs. 2 and 3 demonstrate that the flow rate of streams also considerably affects the efficiency of the MD process. Generally, the efficiency of MD module increases with an increase of the flow rate. This effect is particularly significant for the feed flow rate and is slightly smaller for the distillate flow rate (Gryta et al, 1998, 2000). The effect of the feed flow rate was particularly noticeable in a region of low flow rates. Moreover, the improvement of module efficiency obtained by a variation of the flow rate is limited, since the optimum flow rate of streams exists for each MD module. The experimental results demonstrate that the efficiency of MD module used in the studies (Fig. 3) approaches to a plateau for the feed flow rates above 0.6 m/s.

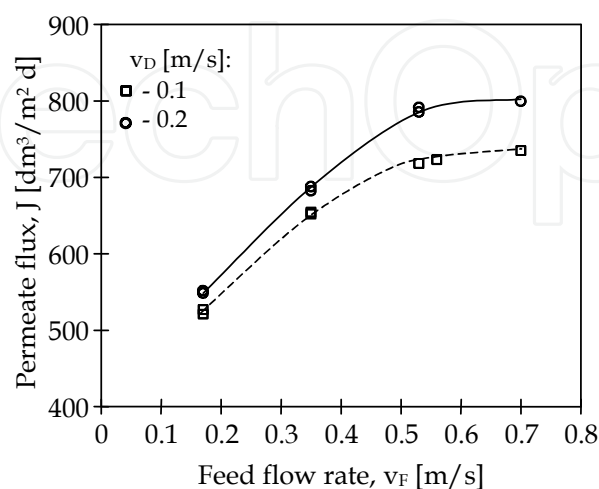


Fig. 3. Influence flow rate of the streams on the MD module efficiency. Module length 1 m,  $T_F=358$  K,  $T_D=293$  K

The observed dependence of permeate flux on the flow rate is essential due to two effects. Firstly, the values of the heat transfer coefficients rise along with an increase of the flow rate, thus a negative influence of temperature polarization decreases. The value of coefficient  $h$  equal to  $5000 \text{ W/m}^2\text{K}$  is considered a threshold value; above this value the effect of temperature polarization may be neglected (Gryta et al, 1998, 2000). This value was achieved at  $v_F$  of about  $0.6 \text{ m/s}$ . Secondly, an enhancement of the flow rate caused that the outlet temperatures of streams were closer to their temperatures at the module entrance (Fig. 4), which also increases the driving force for mass transfer (Gryta, 2002b; Gryta et al., 2000).

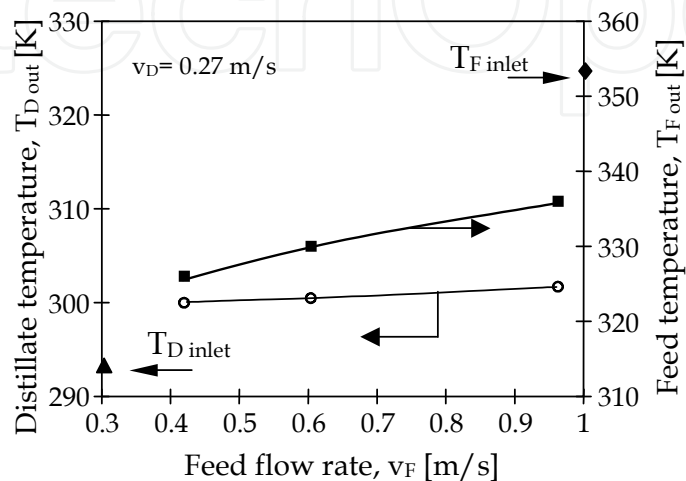


Fig. 4. Influence the feed flow rate on the stream temperature inside the MD module. Module length 1 m, 3 capillary membranes Accurel PP S6/2 arranged inside the  $\frac{1}{2}$  " shell

## 2.2 Heat exchanging between feed and distillate stream

The heat transfer inside the membrane takes place by two possible mechanisms, as conduction across the membrane material ( $Q_C$ ) and as the latent heat associated with vapour diffusing through the membrane ( $Q_V$ ). The amount of heat exchanged in the MD module increases along with an increase of the feed temperature (Fig. 5). However, under these

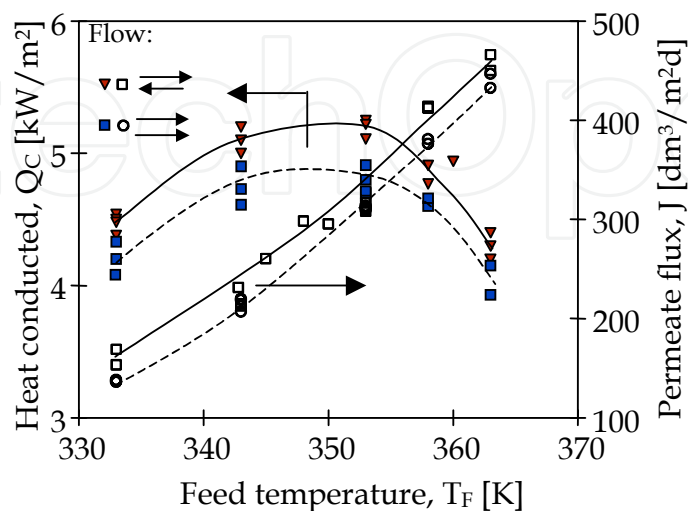


Fig. 5. Influence feed temperature on the MD process efficiency

conditions the permeate flux also increases, which causes the limitation of heat losses (heat conducted through the membrane material). As a result, an increase in the module yield influences on the enhancement of heat efficiency of the MD process and the amount of heat conducted across the membrane ( $Q_C$ ) decreases (Criscuoli et al. 2008; Gryta, 2006b). The streams in MD modules may flow either co-currently, or counter-currently similarly as in the heat exchangers. The larger driving temperature differences can be achieved using the counter-current flow. As a result, an adverse increase in the amount of heat conducted ( $Q_C$ ) take place in the MD process, whereas the permeate flux is only slightly enhanced (Fig.5).

A serious drawback of the counter-current flow is that the flow enables the accumulation of inert gases inside a MD module (Fig.6). The gas bubbles fill the channels hindering the liquid flow and they adhere to the membrane surface, which hinders the mass transfer and

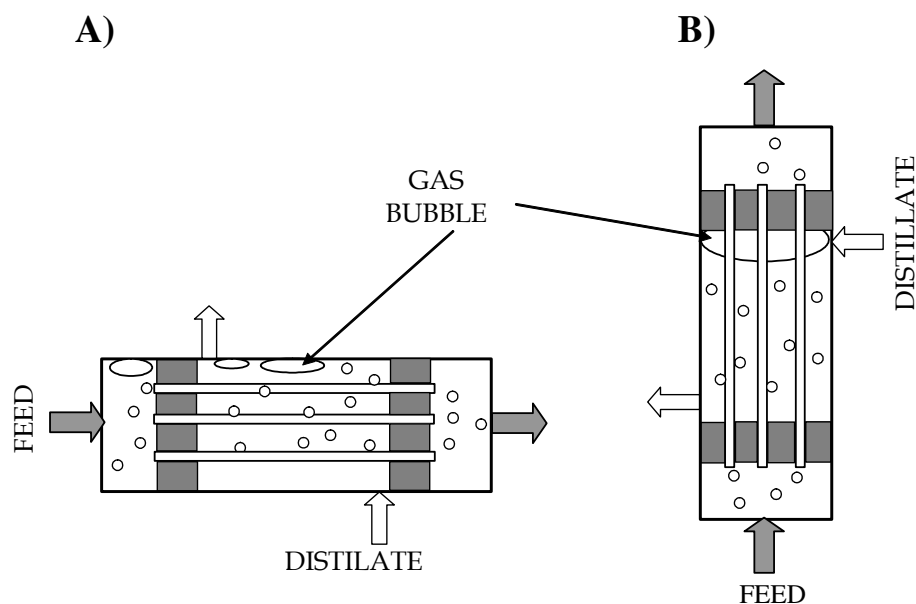


Fig. 6. Accumulation gas bubbles inside the MD modules

as a consequence the MD module efficiency is reduced (Gryta, 2006c). The amount of gases evolved from liquid increases with increasing feed temperature. During the desalination of natural water by MD the desorption of gas from the separated feed is particularly intensive above 343 K. The horizontal arrangement of MD module allows, in a certain degree, to remove a portion of gas bubbles accumulated in the module channels. In the case of module working in a vertical position, the gas will be removed only from the space in which the liquid flows upwards, whereas on the other side of the membrane (e.g. on the shell side - Fig. 6) a volume of entrapped gas phase will be systematically increasing. As a result, the efficiency of module positioned vertically is definitely smaller than that obtained for modules working in a horizontal position (Fig. 7). The inert gases can be removed from the MD installation using degassing of water feeding the membrane module. However, this requires an additional operation that increases the process costs.

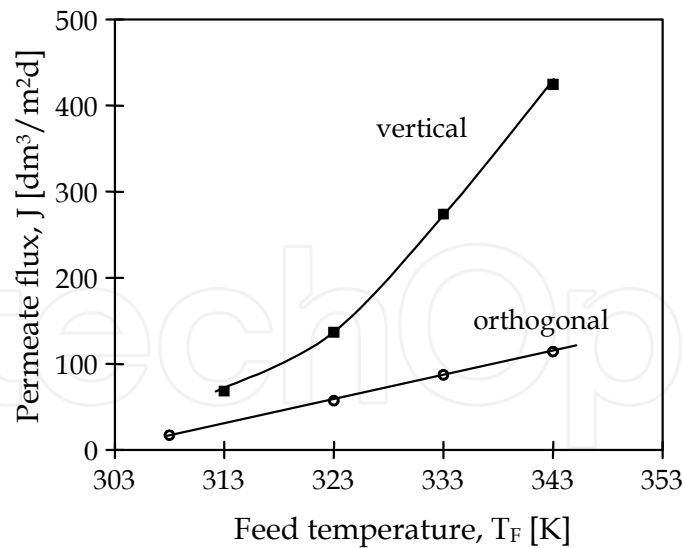


Fig. 7. Influence the position of MD module (vertical or orthogonal) on the permeate flux in the case, when inert gas is accumulated inside the module shell

The problem of inert gases can be solved in a simple way when an additional port-valve is added to the upper part of housing of vertically positioned module (Fig. 8). It enables the removal of inert gases accumulated in the shell of the module. This prevents a decline of the permeate flux and the module efficiency was progressively increased along with increase of feed temperature (Fig. 9). Similarly as before (Fig. 5), the permeate flux for the counter-current flow was only slightly larger than that obtained for the co-current flow. For this reason, it is advantageous to eliminate gas accumulation in the module channels using co-current flow (Gryta, 2005b). In this case the MD module is vertically positioned, and the streams of feed and distillate flows upwards in the module. This allows to remove the bubbles of inert gases formed from MD module in a natural way.

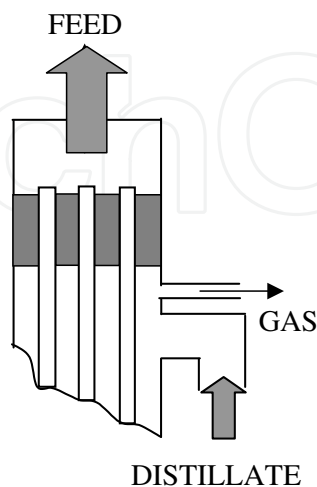


Fig. 8. The design of module head enables to remove inert gas from module shell

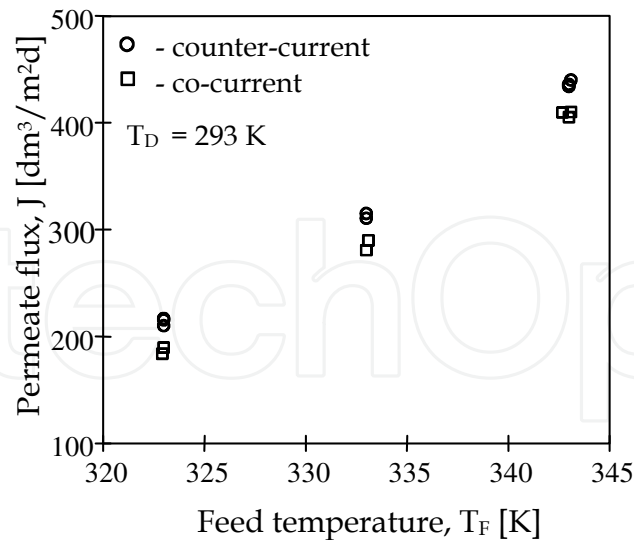


Fig. 9. Influence the feed temperature and direction of streams flow inside the MD module on the permeate flux

### 2.3 Hydrodynamic entrance length

The distance from the channel inlet to the point of the stabilization of laminar velocity profile is defined as the hydrodynamic entrance length (marked as “ $L_H$ ”) (Andersson & Irgens, 1990; Chu-Lien et al., 2010; Doughty & Perkins, 1970; Zhang et al., 2010). Different correlations for the calculation of the Nusselt number are presented in literature for entrance and fully developed flow regions (Gryta et al., 1997, 1998). In the membrane systems often the laminar flow is applied. The membrane modules are relatively short; therefore, the flow development in the entrance region cannot be sometimes omitted. It will be suitable only in the case, when the ratio of the entrance region to the total membrane area is low.

Heat and mass transfer in membrane-formed parallel-plates channels play a key role for performance analysis and system design. The streams flow in the plate-and-frame module is similar to laminar flow inside the rectangular channel. Therefore, the calculation of  $L_H$  entrance length can be made based on the Navier-Stokes equations (Bennett & Myers, 1962; Zhang et al., 2010). For the symmetric channels the growing of hydrodynamic boundary layer is completed when the axial line of duct is reached. The solution of Navier-Stokes equations for the flow between the parallel walls is given by Howarth, and for this case we have (Bennett & Myers, 1962):

$$L_H = 0.015 \text{ Re } h \quad (9)$$

where  $h$  is a high of channel.

A similar relation for analysis of flow inside the broad rectangular channel was obtained, but the coefficient value was 0.04 (Prandtl, 1949). The correlation allowing to calculate the  $L_H$  value for the flow in tubes have a similar form to that presented by equation (9). Most frequently the value of this coefficient is given as equal to 0.03 or 0.0575, whereas the  $\text{Re}$  number is determined for an average flow rate in the tube. The permeate flow through the porous wall influenced on the velocity profile, however, for most membrane processes ( $\text{wall Re} < 1$ ) the analytical solution is sufficient because the symmetric radical of velocity profiles exists.

Parallel-plates channels are the most common structure for plate-and-frame modules. They are simple, and easy to assemble. In plate-and-frame modules usually occur a number of smaller parallel channels instead of one wide channel (Gryta et al., 1997). This caused, that the interaction of side walls also have the influence on the formation of velocity profile. The studies carried out to determine the  $L_H$  value for a channel with width 45 mm and height respectively: 5, 10 and 15 mm gave different results in a comparison with those calculated from Eq.(9). The velocity parabolic profile in XY plane (flow only between parallel plates) was formed earlier, and the observed side-walls effect increases with increasing  $L_H$  values. Due to the side-walls interactions, the hydrodynamic entrance length was established faster, and indicated nonlinear function (Fig. 10). In the rectangular channel the created temporary parabolic profile (plane XY) was transformed into the deformed parabolic profile (plane XYZ).

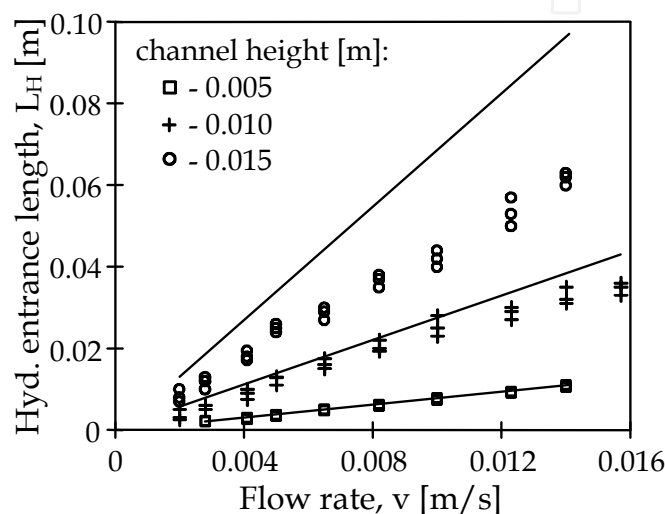


Fig. 10. Variation of hydrodynamic entrance length with flow rate (profile formed in XY plane). Lines – calculated from Eq. (9) described the flow between parallel plates.

According to the theory of boundary layer, the entrance length  $L_H$  is dependent as follows:

$$L_H = f(v_A, v, a, h) \quad (10)$$

where  $a$  is the channel width,  $v_A$  and  $v$  are average flow rate and kinematic viscosity, respectively. Taking into consideration a non-linear form of function and the dimensional analysis, the expected function can be expressed as:

$$L_H = b_1 Re^{b_2} d_h \frac{a}{h} \quad (11)$$

where  $d_h$  is hydraulic diameter.

The  $b_1$  and  $b_2$  coefficients were estimated from the Levenberg-Marquardt Method with minimization of sum of the square deviation. Two hundred of measuring points were used for this analysis. The Snedecors test (F) for significations correlation study has been applied (Volle, 1969). The significance of coefficients study was carried out using Student test (t). In the both tests the signification level has been taken as  $\alpha=0.05$ . The obtained function was as:

$$L_H = 0.069 Re^{0.5} d_h \frac{a}{h} \quad (12)$$

The calculated values of squared coefficient of variation for this equation was 0.95. The results presented in Fig.11 indicated, that the correlation between experimental and calculated data is very good. This confirmed the usefulness of proposed Eq. (12) to calculate the hydrodynamic entrance length under a laminar flow inside the rectangular channel. An estimation of  $L_H$  values gives possibility to calculate the area of entrance region for the plate and frame modules (Zhang et al., 2010).

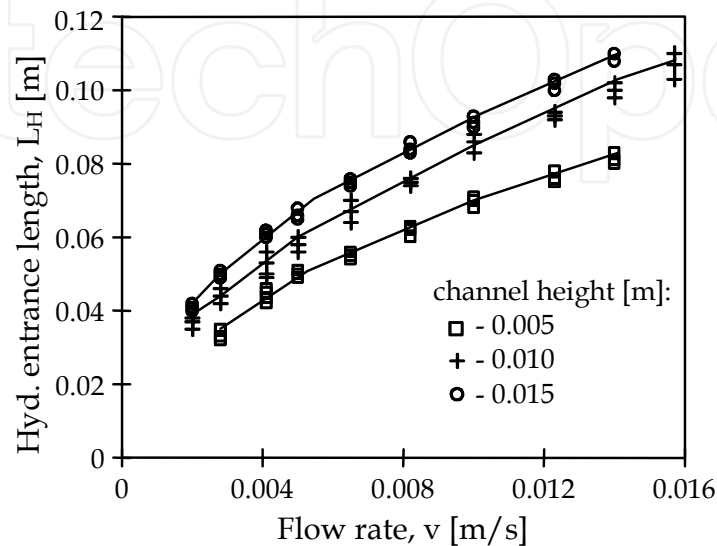


Fig. 11. Variation of hydrodynamic entrance length with velocity for water flow inside rectangular channel (velocity profile formed in XYZ plane). Lines – calculated from Eq. (12)

### 3. Membrane modules for MD process

The availability of the industrial MD modules is currently one of the limitations for MD process implementation. Flat-sheet membranes in plate-and-frame modules or spiral wound modules and capillary membranes in tubular modules have been used in various MD studies (Gryta et al, 2000; Schneider et al., 1988). The design of the MD modules should provide not only good flow conditions, but also has to improve the heat transfer and thermal stability (Teoh et al., 2008; Srisurichan et al., 2006; Phattaranawik et al., 2003).

#### 3.1 Capillary MD modules

The capillary membrane module is a bundle of porous capillaries packed into a shell similar in configuration to a tube-and-shell heat exchanger (Ju-Meng et al., 2004; Schneider et al., 1988). Because of their very high rate of mass transfer, the capillary modules have been used in many practical applications, such as liquid/liquid extraction, artificial kidney, and desalination studies (Singh, 2006). As a thermally driven process, MD can be significantly affected by temperature polarization (Alklaibi & Lior, 2005; El-Bourawi et al., 2006, Su et al., 2010). Among various types of membrane modules, the capillary module shows the least temperature polarization, so it must have a great future in this field (Zhongwei et al., 2003).

In a capillary module used in MD process, the fluid temperatures and transmembrane flux may vary axially alongside the module (Gryta, 2002b). Usually, the feed flows inside the capillary lumen, and distillate flows on the shell side. Theoretically, the capillaries in a bundle can be packed regularly across the shell of a module as in tube-and-shell heat

exchanger. In most industrial modules, however, the distribution of capillary is far more arbitrary; the capillaries are randomly packed in the shell. This leads to a range of duct sizes and shapes in the shell, or the module shows a certain extent variation of the local packing fraction (Gryta et al., 2000; Ju-Meng et al., 2004; Zhongwei et al., 2003). The vast majority of the MD processes occur in the regions with the local packing fraction,  $\varphi$  between 0.3 and 0.6. Production rate (93%) of the module is from these regions, and they occupy only 75% of the overall membrane area of the module. In the regions with  $\varphi$  larger than 0.6, the distillate flow rates are too much smaller than that of the feed, so their temperatures are very close to that of the feed. This means that more than 20% of the feed stream goes through the module almost without any driving force for MD process, so the associated membrane area, more than 20% of the total, is ineffective (Ju-Meng et al., 2004).

A dislocation of the membranes can be limited using a high value of packing fraction  $\varphi$ . However, this caused a reduction of the channel dimensions on the shell side and the increase in the flow resistance, which hinders the application of appropriate high flow rate of distillate. This is an important aspect, because when the distillate flow rate increases, its temperature will become less affected by heat transfer and vapor condensation from the feed side of the membrane, and so does the feed stream. This means that the increment of flow rates can enlarge the temperature difference between these two streams in the module, and in this way the MD process is improved (Zhongwei et al., 2003).

With regards to this, a value of the  $\varphi$  coefficient in MD modules should amount to 0.4-0.6 (Gryta et al., 2000; Ju-Meng et al., 2004; Schneider et al., 1988). In order to limit the changes of capillaries arrangement inside the shell, one should use such assembly of capillaries, which prevents their free displacements. Good results have been obtained by assembling the membrane capillaries inside the sieve baffles or by a tight packing of membranes in a form of braided capillaries (Gryta et al., 2000; Schneider et al., 1988). A comparison of results obtained for the module having the same value of  $\varphi$  coefficient equal to 0.33, but differing in the manner of membranes assembling is presented in Fig. 12. A traditional construction (module M1) based upon the fixation of a bundle of parallel membranes solely at their ends

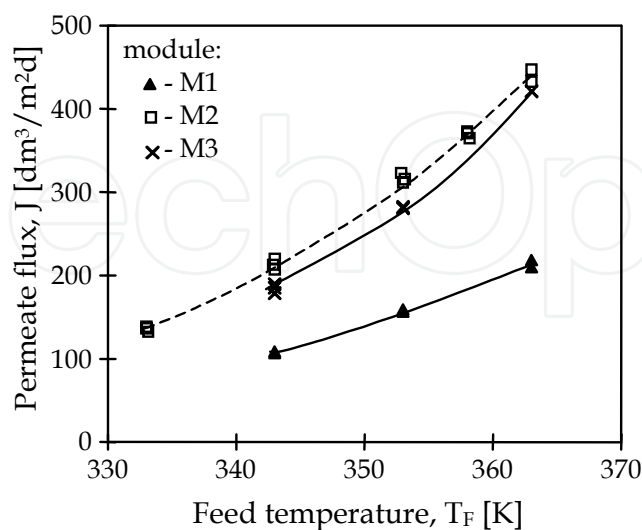


Fig. 12. The influence of feed temperature and the mode of membrane arrangement in a capillary module on the permeate flux. M1 - bundle of parallel membranes; M2 - braided capillaries; and M3 - capillaries mounted inside mesh of sieve baffles

results in that the membranes arrange themselves in a random way. This creates the unfavorable conditions of cooling of the membrane surface by the distillate, which resulted in a decrease of the module efficiency (Gryta et al., 2000; Schneider et al., 1988; Zhongwei et al., 2003). In module M3 the membranes were positioned in every second mesh of six sieve baffles, arranged across the housing with in 0.1–0.15 m. The most advantageous operating conditions of MD module were obtained with the membranes arranged in a form of braided capillaries (module M2). This membrane arrangement improves the hydrodynamic conditions (shape of braided membranes acted as a static mixer), and as a consequence, the module yield was enhanced (Gryta et al., 2000)

A good indicator of the hydrodynamic conditions in a module is the analysis of residence time distribution (RTD). The value of liquid flowing time through the module with good design solution should be closed to the RTD value. The effect of shell-side residence time distribution on mass transfer performance was studied (Lemanski & Lipscomb, 1995). It was pointed out that plug flow would be obtained in an ideal hollow fiber module, but in real shell-side flow the distribution of fluid across the capillary bundle tended to broaden the RTD.

The studies of residence time distribution for a colored impulse in the modules M1-M3 were shown in Figs. 13-14. The RTD value was calculated for assumed plug flow, taking into account a value of  $\varphi=0.34$ . A dye injected into the module appeared the fastest at the outlet of module in the case of module M1 (bundle of parallel capillaries), moreover, the residence time of dye in this module was also the longest. Such result indicates that the non-uniform distribution of capillaries inside the shell caused the formation of channels with different diameters. The distillate was flowing faster in wider channels than the calculated average velocity. As a result, colored water was out flowing faster from the module exit than the calculated RTD value.

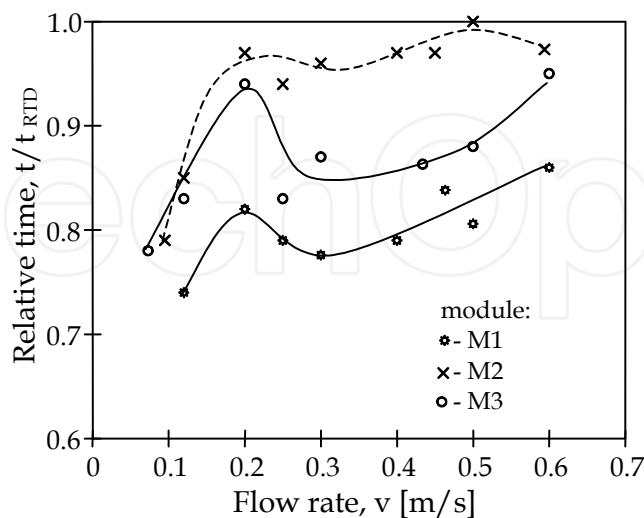


Fig. 13. The influence of flow rate on the relative initial time of colour water residence inside the module. M1 - bundle of parallel membranes; M2 - braided capillaries; and M3 - capillaries mounted inside mesh of sieve baffles

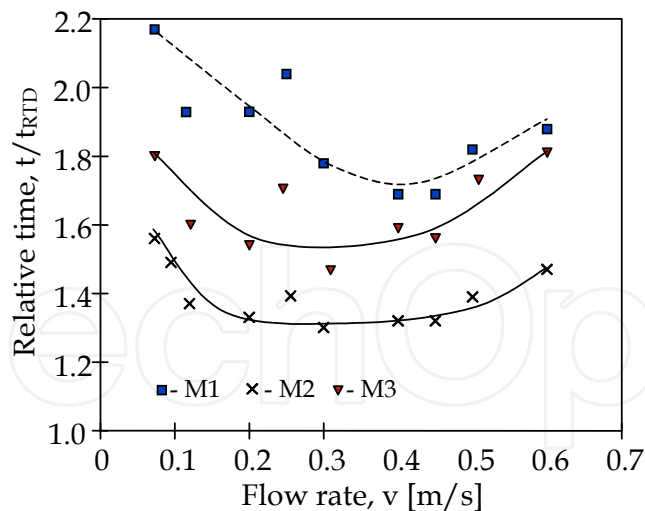


Fig. 14. The influence of flow rate on the total time of dye residence inside the module. M1 - bundle of parallel membranes; M2 - braided capillaries; and M3 - capillaries mounted inside mesh of sieve baffles

As a result of larger values of local capillary packing, the water flows slower in the narrow channels (larger resistance of flow), what prolonged the residence time of dye in the module. An increase in the flow rate increases the turbulence of water flow in the module and dye was washing out faster also from the narrow channels. Due to, the residence time of liquid in the module for larger velocities was closer to the average value. The housings of modules M1-M3 were made of glass tube. This enables the observation of dye spreading out inside their interior. The visual observations of colored streams confirmed these conclusions. The time of water flow in the two remaining modules (M2 and M3) was definitely closer to the RDT value. This indicates, that the dimensions of channels between the capillary membranes had the similar dimension and liquid flows uniformly through the module cross-section. The visual observations also confirmed this fact; dye was uniformly filling up the housing space. The situation was different in the case of module M1, where due to differences in the flow rates, preceded diversity in the intensity of water coloration.

A prolongation of residence time of dye in the module was observed at the flow rates higher than 0.5 m/s. This was associated with growing intensity of liquid mixing in their internal. It was observed, that the vortexes appeared along with the increase in the flow rates. As a result, the portion of colored water were backward transferred, what caused the coloration of new portion of water and due to growing volume of colored water, an apparent longer time of residence in the module was noticed.

### 3.2 Module with flat sheets membranes

The flat sheet membranes are used in the plate-and-frame modules and spiral-wound module design. In the first case, the flat sheet membranes are assembled between the plates having several channels. The membranes are stacked in flow channels connected in series or in parallel. Usually, the plates are rectangular with the flow from one end to the other. The spiral-wound module uses the flat sheet membranes wound around a central tube. The membranes are glued along three sides to form "leaves" A feed channel spacer (a net-like sheet) is placed between the leaves to define the channel height. A three-channel design can be used in the spiral wound module, which allows the recovery of heat transferred from the feed to distillate (Fig.15).

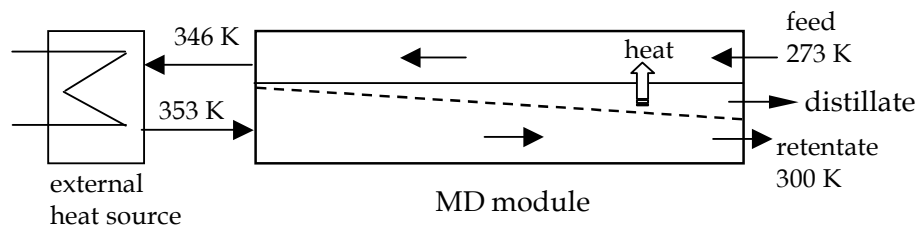


Fig. 15. Module channel arrangement for permeate gap membrane distillation (Winter et al., 2011)

Based on this solution, spiral wound MD modules with a 5-14 m<sup>2</sup> effective membrane area have been developed by Fraunhofer Institute for Solar Energy System (Winter et al., 2011). The cold feed water enters the condenser channel and is heated to approximately 346 K due to internal heat recovery. An external heat source (e.g. solar collector) heats the feed water up to 353 K. The hot feed flows through the evaporator channel in a counter-current direction and exits the module at 300 K. Water vapour passes through the membrane and condenses in the distillate channel. The latent and sensible heat is transferred through the condenser foil to preheat the feed water in the condenser channel. Due to increasing flow resistance, a fast feed flow cannot be used in such a module. As a result, decreasing the vapour pressure with salinity reduces the process driving force. The feed water salinity is considered one of the most important parameters affecting the spiral wound module concept. Larger flow velocities can be used in the plate-and-frame module than in the spiral wound modules. Therefore, the plate-and-frame modules can be utilized for the separation of concentrated salt solutions. The channels in the plate-and-frame modules are shorter; and as a result, an excessive increase of hydraulic pressure is limited. For this reason, several authors suggest the use of spacers as the turbulence promoters (Chu-Lien et al., 2010, Martínez & Rodríguez-Maroto, 2006), because turbulent flow is an appropriate method to decrease the negative effect of polarization phenomena. The turbulent or upper transition flow regime was found in the spacer-filled channels for UF although the Reynolds numbers were still in the laminar regime (Phattaranawik et al., 2003). Net-type spacers are often put into the flow channels in the membrane processes to improve the mass transfer and to reduce the effect of concentration polarization and fouling. The spacers can also be utilized in MD since they destabilize the flow and create eddy currents in the laminar regime so that heat, and mass transfer are enhanced (Teoh et al., 2008; Phattaranawik et al., 2003).

The permeate fluxes obtained from the experiments with spacer-filled channels were compared with those obtained in the experiments performed under laminar and turbulent flow conditions, but for modules with non-filled channels. In the case of experiments with the spacers, a 26-56% increase in the permeate fluxes was achieved, compared with the fluxes performed under laminar flow (Martínez & Rodríguez-Maroto, 2006). However, these fluxes were much lower than those obtained from turbulent flow conditions in the empty channels. This results from the fact, that the feed evaporates during the flow through a module, causing a relatively fast decrease of the feed temperature, which reduces a value of driving force for mass transfer. Thus, in the MD process both the value of the flow rate (m/s) and the volumetric flow (m<sup>3</sup>/s of feed per unit of the membrane area) have a considerable importance. A sufficiently large value of heat transfer coefficient (e.g. 5000 W/m<sup>2</sup>K) allowing to eliminate the temperature polarization, can be generated for laminar

flow (Gryta, 2002b). Although a further increase in the flow rate will not have a substantial influence on the reduction of the temperature polarization, the value of volumetric flow ( $\text{m}^3/\text{s m}^2$ ) will increase significantly, and beneficial results, such as enhancement of the permeate flux, will be obtained.

The nets exhibit the filtration properties, which hinder the use of modules with the channels filled with the nets in certain applications (Fig.16).

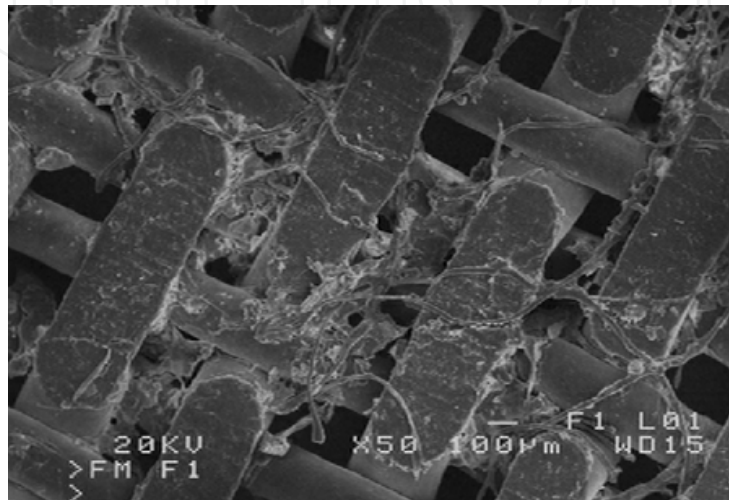


Fig. 16. SEM image of deposit formed inside the net supporting the membrane in the MD module

The concentration of non-clarified juices cannot be carried out with the utilization of such modules (Jiao et al., 2004). The desalination process of hard water, in which significant amounts of  $\text{CaCO}_3$  precipitates are formed (Gryta, 2005a, 2006b), can be another negative exemplary. As demonstrated the nets, favors the hydrogenous crystallization (Gryta, 2009), which would increase the intensity of scaling in the module.

The flat sheet membranes exhibit a low resistance to mechanical damage; therefore, they are reinforced by the application of supporting nets. However, the presence of nets decreases the heat and mass transfer to membrane surfaces, while significantly enhancing the polarization phenomena. These phenomena reduce the difference between  $T_1$  and  $T_2$  interfacial temperatures (Fig. 1), compared to the design when no net was used. Consequently, the driving force for mass transfer is also reduced in the case of net supported membranes. Therefore, a module design in which a part of channel is empty, while a part is filled by net supporting the membrane, significantly influenced reduction of MD efficiency (Gryta et al., 1997).

The module performance can be improved by elimination of nets and by an increase of the number of channels on a module plate so that their walls fill the role of edges supporting the membrane (Fig. 17). It was found that an arrangement of edges every 15-20 mm was appropriate for the membranes made of PVDF and PTFE with the thickness of 100-150  $\mu\text{m}$  (Gryta et al., 1997; Tomaszewska et al., 2000).

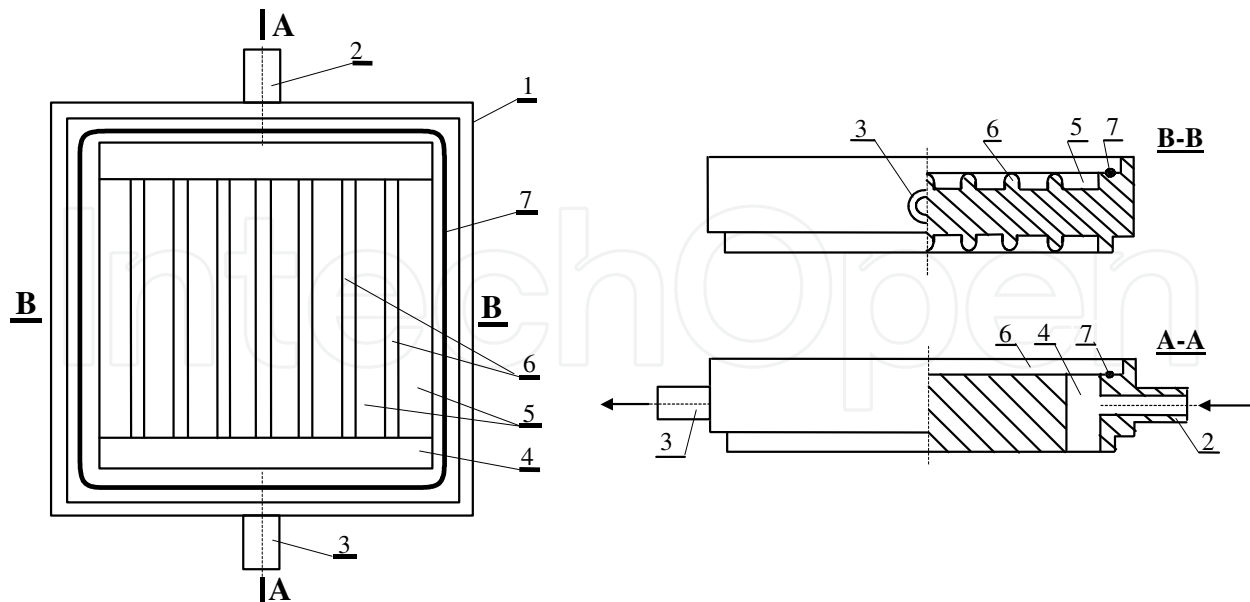


Fig. 17. Plate-and-frame MD module design. 1 - module plate, 2 - inlet channel, 3 - outlet channel, 4 - lateral feeding channel, 5 - distribution channels, 6 - edges supporting the membrane, 7 - o-ring

The individual plates of the module possess a series of channels connected most frequently with one feeding channel. As the pressure in this channel increases along with the increase in the flow rate, it may lead to membrane damage in this region. This problem was solved by placing an inlet opening of feeding channel below a plane of the distribution channels, which were connected by an additional lateral channel (Fig.17). As a result, liquid with large velocity flew out from the inlet channel and spreads on sides in the lateral channel. As its cross-section is several times larger, liquid flow rate slows down and flows into the distribution channels with a lower energy (Fig. 18).

A visualization of feed flow in the distribution channel of the plate-and-frame module with a central one-point feeding of the plate was shown in Fig. 19.

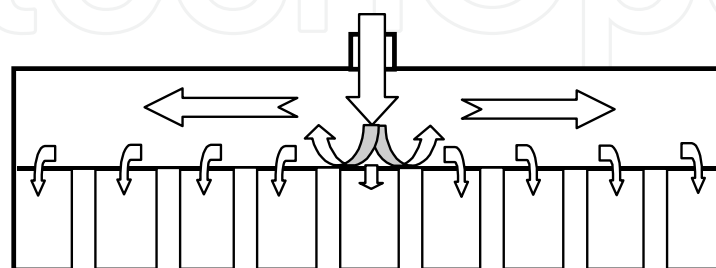


Fig. 18. The schema of water flow inside the distribution channel of the plate-and-frame module presented in Fig. 17

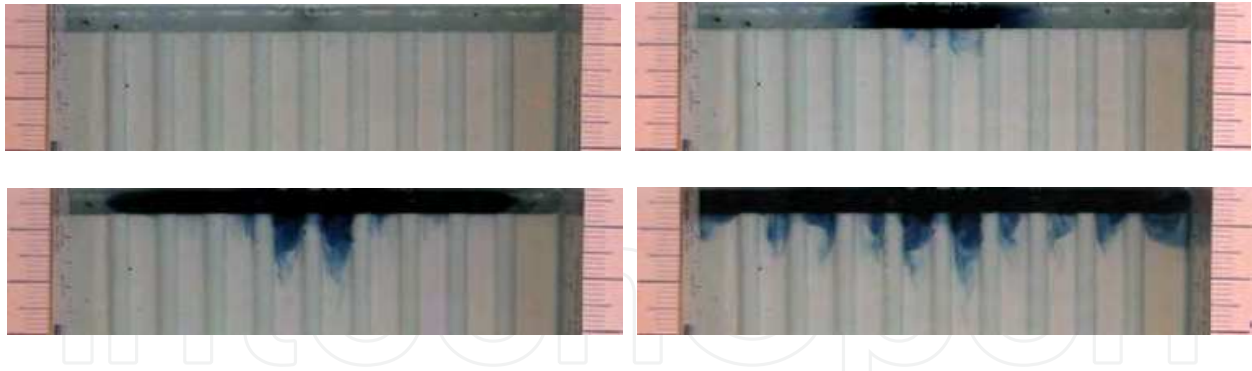


Fig. 19. A visualization of feed flow in the distribution channel

### 3.2.1 Uniformity of flow

In the capillary modules good conditions of mixing and a flow close to plug flow can be achieved by using an appropriate design, e.g. by assembling the braided capillaries. However, the achievement of uniform flow of liquid throughout the entire cross-section of plate-and-frame modules is definitely more difficult. As a rule, one can expect different flow rates in the particular channels. The studies have demonstrated that this variability is dependent not only on the location of channels, but also on the rate of module feeding. A visualization of variations in the flow rates of liquid in the particular channels of the module with a central one-point feeding of plate was shown in Figs. 19 and 20. The larger is the fraction of a given channel filled with colored water, the larger is the flow rate of liquid in this channel (relative for each case). In these studies, a module was feed with a flow rate of 0.1-0.86 dm<sup>3</sup>/min, which corresponds to the average flow rate of 0.007-0.06 m/s. The obtained results indicate that the highest flow rate was achieved in the terminal channels, whereas the lowest rate was obtained in the module axis. This tendency was growing along with an increase in the supply flow. Most likely, a slight increase in the middle channel width would reduce the flow rate resistance, and as a result, cause a larger uniformity of flow rate distribution across the entire plate of the module.



A) feeding 0.1 dm<sup>3</sup>/min

B) feeding 0.21 dm<sup>3</sup>/min

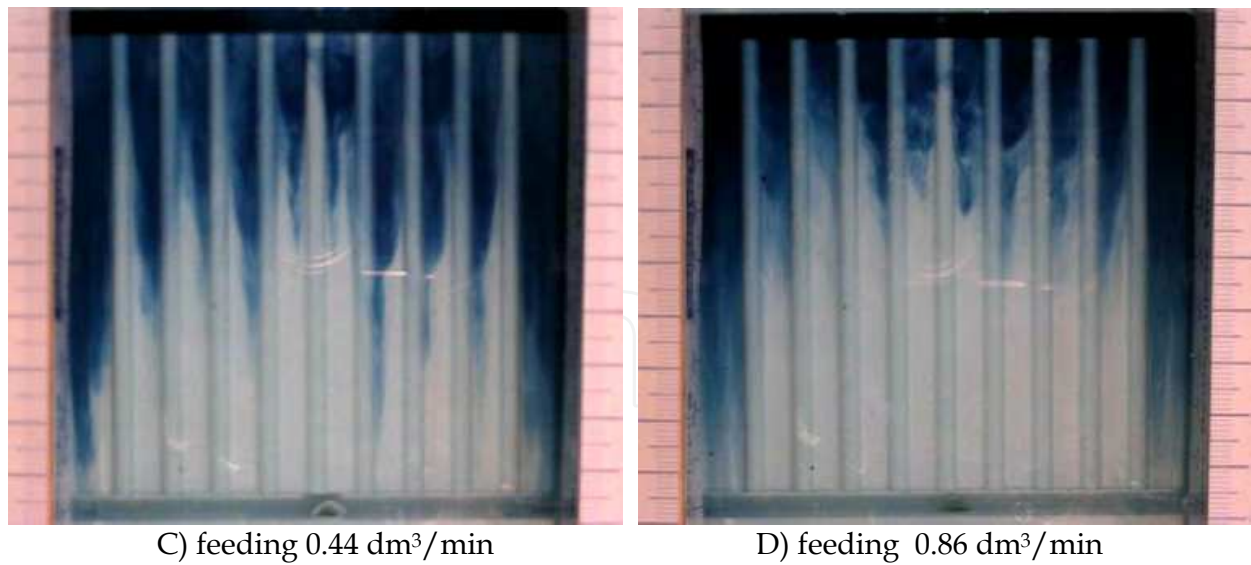
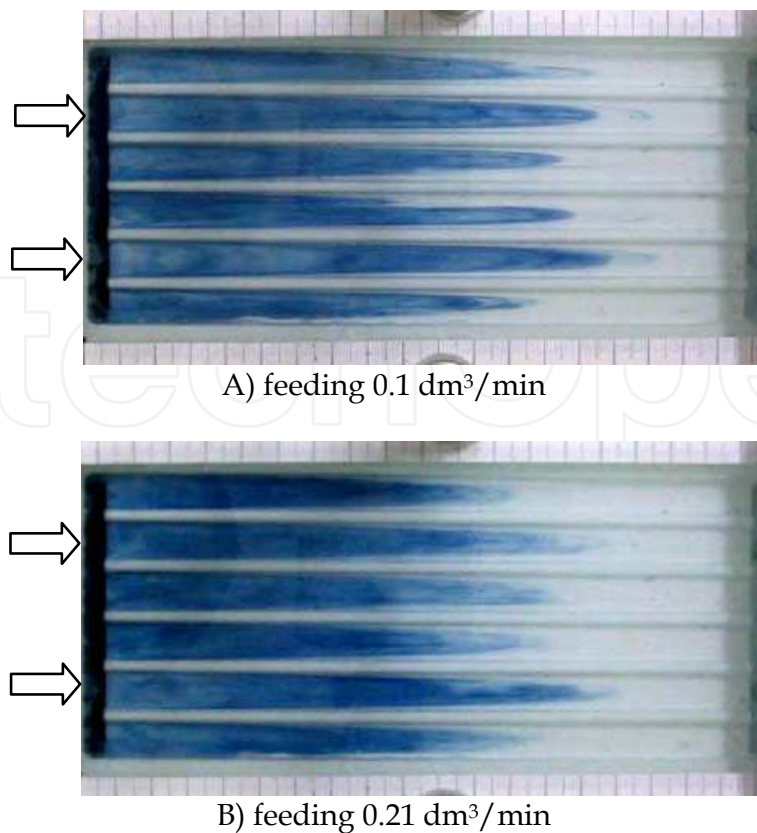


Fig. 20. Visualization of variations in the flow rates of water (302 K) in the particular channels of the module (channel dimension 6x3.9 mm) with a central one-point feeding of plate

A substantial improvement in the flow uniformity was achieved when the water was feed into the feeding channel in two places (Fig. 21). In this case, the connections were assembled in a distance of  $\frac{1}{4}$  plate width from each end of the channel. The module was



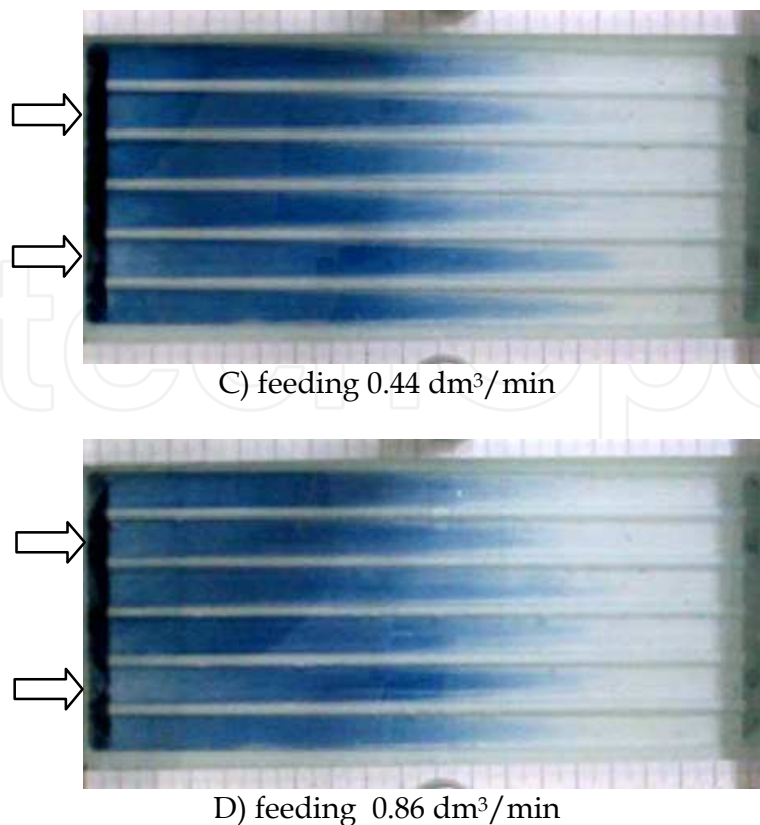


Fig. 21. Visualization of variations in the flow rates of water (302 K) in the particular channels of the module (channel dimension 10x3.5 mm) with a two-point feeding of module plate

feeding with the flow rate of 0.1-0.86 dm<sup>3</sup>/min, which corresponds to the average flow rate 0.008-0.07 m/s. The presented pictures indicate that a velocity profile characteristic for the laminar flow can be observed only for a very slow flow (0.008 m/s). An increase in the uniformity of liquid coloration in the channels was observed at larger supply flows what indicates for a flow close to the plug flow. Most probably this effect was obtained due to an increase in the turbulent flow of liquid in the feeding channel. This may equalize the hydraulic pressure along this channel, and cause liquid to flow more uniformly into the distribution channels.

#### 4. Conclusions

The driving force of MD depends, in a significant degree, on turbulence of stream flow in the membrane module. Therefore, the hydrodynamic conditions existing in the module have a large influence on the MD process efficiency. Just as in the modules used for pressure-driven processes, it is important to minimize the flow resistance through the MD module channels. However, the reason for this was different, because the pressure drop is not limited, rather, the hydraulic pressure should be as low as possible, so as to restrict the membrane wettability.

The maintenance of adequately high flow rates limits the concentration polarization and fouling, but in the case of MD modules the magnitude of temperature polarization also has a

substantial influence. The latter polarization can be significantly reduced when the flow turbulence yield a heat transfer coefficient above  $5000 \text{ W/m}^2\text{K}$ . This coefficient is affected by the value of the flow rate as well as by the design of flow channels. The filling of channels with nets or an arrangement of braided capillary membranes ensures an increase in the flow turbulence and good conditions for heat transfer can be achieved at lower values of flow rates. Therefore, in the case of MD modules construction, one should consider design requirements typical for pressure driven membrane processes as well as a necessity to ensure the appropriate conditions for heat transfer.

The efficiency of MD capillary modules is significantly affected by the manner in which the membranes are arranged within a housing. A traditional construction based upon the fixation of a bundle of parallel membranes solely at their ends causes that the membranes arranged themselves in a random way. This creates unfavorable conditions of cooling of the membrane surface by the distillate; hence, the module efficiency is reduced due to the enhancement of temperature polarization. On the other hand, arranging the membranes in a way to ensure a uniform distribution over the module cross-section (braided membranes or supported by sieve baffles alongside module) increases the efficiency over 100%.

The feed temperature in MD module decreases due to the evaporation, which also causes a reduction of MD driving force, besides the temperature polarization. Therefore, the permeate flux can be increased several times when the feed outlet temperature is closed to its inlet temperature, which is obtained by increasing the flow rate. The optimal value of the flow rate for several studied modules amounts to  $0.6\text{--}1 \text{ m/s}$  and  $0.4\text{--}0.7 \text{ m/s}$  for feed and distillate, respectively.

## 5. References

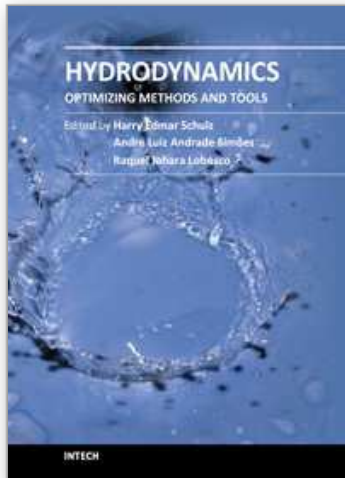
- Alklaibi, A.M. & Lior, N. (2005). Membrane-distillation desalination: status and potential, *Desalination*, Vol.171, No.2, (January 2005), pp. 111–131, ISSN 0011-9164
- Andersson, H.I. & Irgens, F. (1990) Hydrodynamic entrance length of non-newtonian liquid films. *Chemical Engineering Science*, Vol.45, No.2, (January 1990), pp. 537–541, ISSN 0009-2509
- Banat, F. & Jwaied, N. (2008). Economic evaluation of desalination by small-scale autonomous solar-powered membrane distillation units. *Desalination*, Vol.220, No.1-3, (March 2008), pp. 566–573, ISSN 0011-9164
- Bennett, C.O. & Myers, J.E. (1982). *Momentum, heat and mass transport* (3 rd ed.), Mc Grow-Hill Book Company, ISBN 0070046719, New York, USA
- Bonyadi, S. & Chung, T.S. (2009). Highly porous and macrovoid-free PVDF hollow fiber membranes for membrane distillation by a solvent-dope solution co-extrusion approach, *Journal of Membrane Science*, Vol.331, No.1-2, (April 2009), pp. 66–74, ISSN 0376-7388
- Bui, V.A.; Vu, L.T.T. & Nguyen, M.H. (2010). Simulation and optimization of direct contact membrane distillation for energy efficiency. *Desalination*, Vol.259, No.1-3, (September 2010), pp. 29–37, ISSN 0011-9164
- Chu-Lien, L.; Yu-Feng, Ch.; Wen-Junn, S. & Chi-Chuan, W. (2010). Effect of flow deflector on the flux improvement in direct contact membrane distillation. *Desalination*, Vol.253, (April 2010), pp. 16–21, ISSN 0011-9164

- Criscuoli, A.; Carnevale, M.C. & Drioli, E. (2008). Evaluation of energy requirements in membrane distillation, *Chemical Engineering and Processing*, Vol.47, No.7, (July 2008), pp. 1098-1105, ISSN 0009-2509
- Drioli, E.; Curcio, E.; Criscuoli, A. & Di Profio, G. (2004). Integrated system for recovery of  $\text{CaCO}_3$ ,  $\text{NaCl}$ ,  $\text{MgSO}_4 \cdot 7\text{H}_2\text{O}$  from nanofiltration retentate, *Journal of Membrane Science*, Vol.239, No.1, (August 2004), pp. 27-38, ISSN 0376-7388
- Doughty, J.R. & Perkins JR, H.C. (1970). Hydrodynamic entry length for laminar flow between parallel porous plates. *Journal of Applied Mechanics*. Vol.37, (May 1970), pp. 548, ISSN 0021-8936
- El-Bourawi, M.S.; Ding, Z.; Ma, R & Khayet, M. (2006). A framework for better understanding membrane distillation separation process. *Journal of Membrane Science*, Vol.285, No.1-2, (November 2006), pp. 4-29, ISSN 0376-7388
- Gryta, M.; Tomaszewska, M. & Morawski, A.W. (1997). Membrane distillation with laminar flow. *Separation and Purification Technology*, Vol.11, No.2, (June 1997), pp. 93-101, ISSN 1383-5866
- Gryta, M.; Tomaszewska, M. & Morawski, W. (1998). Heat transport in the membrane distillation process, *Journal of Membrane Science*, Vol.144, No.1-2, (June 1998), pp. 211-222, ISSN 0376-7388
- Gryta, M.; Tomaszewska, M. & Morawski, A.W. (2000). A capillary module for membrane distillation process, *Chemical Papers*, Vol.54, No.6a, (July 2000), pp. 370-374, ISSN 0366-6352
- Gryta, M. (2002a). Direct contact membrane distillation with crystallization applied to  $\text{NaCl}$  solutions, *Chemical Papers*, Vol.56, No.1, (January 2002), pp. 14-19, ISSN 0366-6352
- Gryta, M. (2002b). Concentration of  $\text{NaCl}$  solution by membrane distillation integrated with crystallization. *Separation Science and Technology*. Vol.37, No.15, (November 2002), pp. 3535-3558, ISSN 0149-6395
- Gryta, M. (2005a). Osmotic MD and other membrane distillation variants. *Journal of Membrane Science*, Vol.246, No.2, (January 2005), pp.45-56, ISSN 0376-7388
- Gryta, M. (2005b). Long-term performance of membrane distillation process, *Journal of Membrane Science*., Vol.265, No.1-2, (November 2005), pp. 153-159, ISSN 0376-7388
- Gryta, M. (2006a). Water purification by membrane distillation process, *Separation Science and Technology*. Vol.41, No.9, (September 2006), pp. 1789-1798, ISSN 0149-6395
- Gryta, M. (2006b). Heat efficiency of the capillary modules for membrane distillation process, *Inżynieria Chemiczna i Procesowa*, Vol.27, No.1, (January 2006), pp. 305-314, ISSN 0208-6425
- Gryta M. (2006c). Deaeration capillary modules during membrane distillation (in Polish). *Inżynieria i Aparatura Chemiczna*, Vol.45, No.3, (June 2006), pp. 20-23, ISSN 0368-0827
- Gryta, M. (2008). Fouling in direct contact membrane distillation process, *Journal of Membrane Science*, Vol.325, No.1, (November 2008), pp. 383-394, ISSN 0376-7388
- Gryta, M. (2009). Scaling diminution by heterogeneous crystallization in a filtration element integrated with membrane distillation module, *Polish Journal of Chemical Technology*, Vol.11, No.1, (February 2009), pp. 59-64, ISSN 1509-8117
- Gryta, M. & Barancewicz, M. (2010). Influence of morphology of PVDF capillary membranes on the performance of direct contact membrane distillation, *Journal of Membrane Science*, Vol.358, No.1-2, (August 2010), pp. 158-167, ISSN 0376-7388

- Gryta, M. (2010a). Application of membrane distillation process for tap water purification. *Membrane Water Treatment*, Vol.1, No.1 (January 2010), pp. 1-12, ISSN 2005-8624
- Gryta, M. (2010b). Desalination of thermally softened water by membrane distillation process. *Desalination*, Vol.257, No.1-3 (July 2010), pp. 30-35, ISSN 0011-9164
- Jiao, B.; Cassano, A. & Drioli, E. (2004). Recent advanced on membrane processes for the concentration of fruit juices: a review, *Journal of Food Engineering*, Vol.63, No.3 (August 2004), pp. 303-324, ISSN 0260-8774
- Ju-Meng, Z.; Zhi-Kang, X.; Jian-Mei, L.; Shu-Yuan, W. & You-Yi, X. (2004). Influence of random arrangement of hollow fiber membranes on shell side mass transfer performance: a novel model prediction. *Journal of Membrane Science*, Vol.236, No.1-2, (June 2004), pp. 145-151, ISSN 0376-7388
- Karakulski, K.; Gryta, M. & Sasim, M. (2006). Production of process water using integrated membrane processes, *Chemical Papers*, Vol.60, No.6, (November 2006), pp. 416-421, ISSN 0366-6352
- Khayet, M.; Godino, M.P. & Mengual, J.I. (2004). Study of asymmetric polarization in direct contact membrane distillation, *Separation Science and Technology*, Vol.39, No.1 (January 2004), pp. 125-147, ISSN 0149-6395
- Lawson, K.W. & Lloyd, D.R. (1997). Membrane distillation. *Journal of Membrane Science*, Vol.124, No.1, (February 1997), pp. 1-25, ISSN 0376-7388
- Lemanski, J. & Lipscomb, G.G. (1995). Effect of shell-side flows on hollow fiber membrane device performance, *American Institute of Chemical Engineering Journal*. Vol.41, No.10, (October 1995), pp. 2322-2326, ISSN 1547-5905
- Li, B. & Sirkar, K.K. (2004). Novel membrane and device for direct contact membrane distillation-based desalination process, *Industrial Engineering Chemical Research*, Vol.43, No.17, (August 2004), pp. 5300-5309, ISSN 0888-5885
- Martínez-Díez, L. & Vázquez-González, M.I. (1999). Temperature and concentration polarization in membrane distillation of aqueous salt solutions, *Journal of Membrane Science*, Vol.156, No.2, (April 1999), pp. 265-273, ISSN 0376-7388
- Martínez, L. & Rodríguez-Maroto, J.M. (2006). Characterization of membrane distillation modules and analysis of mass flux enhancement by channel spacers. *Journal of Membrane Science*, Vol.274, No.1-2, (April 2006), pp. 123-137, ISSN 0376-7388
- Phattaranawik, J.; Jiraratananon, R. & Fane, A.G. (2003). Heat transport and membrane distillation coefficients in direct contact membrane distillation, *Journal of Membrane Science*, Vol.212, No.1-2 (February 2003), pp. 177-193, ISSN 0376-7388
- Prandtl, L. (1949). *Führer durch die Stromungslehre*. Friedrich Vieweg u. Sohn, Braunschweig, Germany
- Schneider, K.; Hölz, W. & Wollbeck, R. (1988). Membranes and modules for transmembrane distillation, *Journal of Membrane Science*, Vol.39, No.1, (October 1988), pp. 25-42, ISSN 0376-7388
- Singh, R (2006). *Hybrid Membrane Systems for Water Purification*, Elsevier, ISBN 1-856-17442-5, Kidlington, UK
- Schofield, R.W.; Fane, A.G.; Fell, C.J.D. & Macoun, R. (1990). Factors affecting flux in membrane distillation. *Desalination*, Vol.77, (March 1990), pp. 279-294, ISSN 0011-9164
- Srisurichan, S.; Jiraratananon, R. & Fane, A.G. (2005). Humic acid fouling in the membrane distillation, *Desalination*, Vol.174, No.1, (April 2005), pp. 63-72, ISSN 0011-9164

- Srisurichan, S.; Jiratananon, R. & Fane, A.G. (2006). Mass transfer mechanisms and transport resistances in direct contact membrane distillation process, *Journal of Membrane Science*, Vol.277, No.1-2, (June 2006), pp. 186–194, ISSN 0376-7388
- Su, M.; Teoh, M.M.; Wang, K.Y.; Su, J. & Chung, T.S. (2010), Effect of inner-layer thermal conductivity on flux enhancement of dual-layer hollow fiber membranes in direct contact membrane distillation. *Journal of Membrane Science*, Vol.364, No.1-2, (November 2010), pp. 278–289, ISSN 0376-7388
- Teoh, M.M.; Bonyadi, S. & Chung, T.S. (2008). Investigation of different hollow fiber module designs or flux enhancement in the membrane distillation process, *Journal of Membrane Science*, Vol.311, No.1-2, (March 2008), pp. 371–379, ISSN 0376-7388
- Tomaszewska M.; Gryta, M. & Morawski, A.W. (2000). Mass transfer of HCl and H<sub>2</sub>O across the hydrophobic membrane during membrane distillation. *Journal of Membrane Science*, Vol.166, No.2, (February 2000), pp. 149–157, ISSN 0376-7388
- Wang, K.Y.; Chung, T.S. & Gryta, M. (2008). Hydrophobic PVDF hollow fiber membranes with narrow pore size distribution and ultra-thin skin for the freshwater production through membrane distillation, *Chemical Engineering Science*, Vol.63, No.9, (May 2008), pp. 2587–2594, ISSN 0009-2509
- Winter, D.; Koschikowski, J. & Wieghaus, M. (2011). Desalination using membrane distillation: Experimental studies on full scale spiral wound modules. *Journal of Membrane Science*, Vol.375, No.1-2 (June 2011), pp. 104–112, ISSN 0376-7388
- Volk, W. *Applied statistics for engineers* (1969), McGraw-Hill, ISBN 0070675511, New York, USA
- Zhang, L.Z.; Liang, C.H. & Pei, L.X. (2010). Conjugate heat and mass transfer in membrane-formed channels in all entry regions. *International Journal of Heat and Mass Transfer*, Vol.53, No.5, (February 2010), pp. 815–824. ISSN 0017-9310
- Zhongwei, D.; Liying, L. & Runyu, M. (2003). Study on the effect of flow maldistribution on the performance of the hollow fiber modules used in membrane distillation. *Journal of Membrane Science*, Vol.215, No.1-2, (April 2003), pp. 11–23, ISSN 0376-7388

IntechOpen



## Hydrodynamics - Optimizing Methods and Tools

Edited by Prof. Harry Schulz

ISBN 978-953-307-712-3

Hard cover, 420 pages

**Publisher** InTech

**Published online** 26, October, 2011

**Published in print edition** October, 2011

The constant evolution of the calculation capacity of the modern computers implies in a permanent effort to adjust the existing numerical codes, or to create new codes following new points of view, aiming to adequately simulate fluid flows and the related transport of physical properties. Additionally, the continuous improving of laboratory devices and equipment, which allow to record and measure fluid flows with a higher degree of details, induces to elaborate specific experiments, in order to shed light in unsolved aspects of the phenomena related to these flows. This volume presents conclusions about different aspects of calculated and observed flows, discussing the tools used in the analyses. It contains eighteen chapters, organized in four sections: 1) Smoothed Spheres, 2) Models and Codes in Fluid Dynamics, 3) Complex Hydraulic Engineering Applications, 4) Hydrodynamics and Heat/Mass Transfer. The chapters present results directed to the optimization of the methods and tools of Hydrodynamics.

### How to reference

In order to correctly reference this scholarly work, feel free to copy and paste the following:

Marek Gryta (2011). The Influence of the Hydrodynamic Conditions on the Performance of Membrane Distillation, Hydrodynamics - Optimizing Methods and Tools, Prof. Harry Schulz (Ed.), ISBN: 978-953-307-712-3, InTech, Available from: <http://www.intechopen.com/books/hydrodynamics-optimizing-methods-and-tools/the-influence-of-the-hydrodynamic-conditions-on-the-performance-of-membrane-distillation>

**INTECH**  
open science | open minds

### InTech Europe

University Campus STeP Ri  
Slavka Krautzeka 83/A  
51000 Rijeka, Croatia  
Phone: +385 (51) 770 447  
Fax: +385 (51) 686 166  
[www.intechopen.com](http://www.intechopen.com)

### InTech China

Unit 405, Office Block, Hotel Equatorial Shanghai  
No.65, Yan An Road (West), Shanghai, 200040, China  
中国上海市延安西路65号上海国际贵都大饭店办公楼405单元  
Phone: +86-21-62489820  
Fax: +86-21-62489821

© 2011 The Author(s). Licensee IntechOpen. This is an open access article distributed under the terms of the [Creative Commons Attribution 3.0 License](#), which permits unrestricted use, distribution, and reproduction in any medium, provided the original work is properly cited.

IntechOpen

IntechOpen